

# miR-543 and miR-590-3p regulate human mesenchymal stem cell aging via direct targeting of AIMP3/p18

Seunghye Lee · Kyung-Rok Yu · Young-Sil Ryu · Young Sun Oh · In-Sun Hong · Hyung-Sik Kim · Jin Young Lee · Sunghoon Kim · Kwang-Won Seo · Kyung-Sun Kang

Received: 5 March 2014 / Accepted: 22 October 2014  
© American Aging Association 2014

**Abstract** Previously, AIMP3 (aminoacyl-tRNA synthetase-interacting multifunctional protein-3) was shown to be involved in the macromolecular tRNA synthetase complex or to act as a tumor suppressor. In this study, we report a novel role of AIMP3/p18 in the cellular aging of human mesenchymal stem cells (hMSCs). We found that AIMP3/p18 expression significantly increased in senescent hMSCs and in aged mouse bone marrow-derived MSCs (mBM-MSCs). AIMP3/p18 overexpression is sufficient to induce the

cellular senescence phenotypes with compromised clonogenicity and adipogenic differentiation potential. To identify the upstream regulators of AIMP3/p18 during senescence, we screened for potential epigenetic regulators and for miRNAs. We found that the levels of miR-543 and miR-590-3p significantly decreased under senescence-inducing conditions, whereas the AIMP3/p18 protein levels increased. We demonstrate for the first time that miR-543 and miR-590-3p are able to decrease AIMP3/p18 expression levels through direct

Seunghye Lee and Kyung-Rok Yu contributed equally to this work.

**Electronic supplementary material** The online version of this article (doi:10.1007/s11357-014-9724-2) contains supplementary material, which is available to authorized users.

S. Lee · K.-R. Yu · Y.-S. Ryu · H.-S. Kim · J. Y. Lee · K.-W. Seo (✉) · K.-S. Kang (✉)  
Adult Stem Cell Research Center, College of Veterinary Medicine, Seoul National University,  
Seoul 151-742, Republic of Korea  
e-mail: kwang\_wons@hotmail.com  
e-mail: kangpub@snu.ac.kr

S. Lee · K.-R. Yu · Y.-S. Ryu · H.-S. Kim · J. Y. Lee · K.-W. Seo · K.-S. Kang  
Research Institute for Veterinary Medicine, College of Veterinary Medicine, Seoul National University,  
Seoul 151-742, Republic of Korea

S. Lee · H.-S. Kim · K.-W. Seo  
Institute for Stem Cell and Regenerative Medicine in Kang Stem Biotech, Biotechnology Incubating Center, Seoul National University,  
Seoul 151-742, Republic of Korea

Y. S. Oh · S. Kim  
Medicinal Bioconvergence Research Center, Seoul National University,  
Seoul 151-742, Republic of Korea

Y. S. Oh · S. Kim  
WCU Department of Molecular Medicine and Biopharmaceutical Sciences, Graduate School of Convergence Science and Technology, Seoul National University,  
Suwon 443-270, Republic of Korea

I.-S. Hong  
Department of Molecular Medicine, Gachon University,  
Incheon, Republic of Korea

I.-S. Hong  
Lee Gil Ya Cancer and Diabetes Institute,  
Incheon, Republic of Korea

binding to the AIMP/p18 transcripts, which further compromised the induction of the senescence phenotype. Taken together, our data demonstrate that AIMP3/p18 regulates cellular aging in hMSCs possibly through miR-543 and miR-590-3p.

**Keywords** AIMP3/p18 · Stem cell · Aging · miR-543 · miR-590-3p

### Abbreviations

AIMP3	aminoacyl-tRNAsynthetase-interacting multifunctional protein-3
MSCs	mesenchymal stem cells
hUCB	human umbilical cord blood
mBM	mouse bone marrow
miRNAs	microRNAs
MRS	methionyl-tRNAsynthetase
SA- $\beta$ -gal	senescence-associated $\beta$ -galactosidase
ICC	immunocytochemistry
WT	wild type
TG	transgenic
VPA	valproic acid
SB	sodium butyrate
5-azaC	5-azacytidine
AceH4	acetyl histone H4
H3K4Me3	histone H3 lysine 4 trimethylation
H3K27Me3	histone H3 lysine 27 trimethylation

### Introduction

Aminoacyl-transfer RNA (tRNA) synthetases (ARSs) are enzymes that catalyze the ligation of a specific amino acid to its compatible cognate tRNA to form an aminoacyl-tRNA. ARS-interacting multi-functional proteins (AIMPs) are non-enzymatic factors that serve as molecular reservoirs that harbor ARSs until being dispatched to target sites (Kim et al. 2011). AIMP3/p18 is the smallest member of the AIMP family, which includes AIMP1/p43, AIMP2/p38, and AIMP3/p18. AIMP3/p18 is normally associated with the multi-synthetase complex via its specific interaction with methionyl-tRNA synthetase (MRS), which facilitates the delivery of a methionine-charged initiator tRNA from MRS to the initiation factor complex (Kang et al. 2012). Recently, the function of AIMP3/p18 has been elucidated using genetically modified mouse models. *Aimp3/p18* null knockout mice are early embryonic

lethal, which highlight the importance of AIMP3/p18 during developmental processes (Park et al. 2005). *Aimp3/p18* heterozygous knockout (HKO) mice exhibit no developmental defects; however, these mice spontaneously develop various cancers at approximately 15 months after birth (Park et al. 2005). AIMP3/p18 functions as a tumor suppressor by controlling the growth factor- or Ras-dependent induction of p53 (Park et al. 2006). Although the inhibition of AIMP3/p18 expression promoted tumorigenesis, the forced expression of AIMP3/p18 induced cellular senescence through specific down-regulation of mature lamin A. Moreover, *Aimp3/p18* transgenic mice exhibited progeria-like phenotypes (Oh et al. 2010). These results suggest that AIMP3/p18 plays a significant role in tumorigenesis regulation and in aging. However, the precise role of AIMP3/p18 during the aging process of adult stem cells such as hMSCs has not yet been described.

Thus far, several hypotheses regarding the mechanisms of the aging process have been presented. Hayflick (1965) suggested that normal diploid cells lose their ability to divide after approximately 50 cell divisions; this reduction in cell proliferation capability, along with enlargement, morphological changes, and senescence-associated  $\beta$ -galactosidase (SA- $\beta$ -gal) expression after repeated divisions, is known as replicative senescence or the Hayflick phenomenon (Olovnikov 1996). In addition to replicative senescence, ionizing radiation, DNA-damaging drugs such as mitomycin C, oxidative stress, and histone acetylase inhibitors can trigger premature cellular senescence (Blagosklonny 2003; Chang et al. 1999; Itahana et al. 2001; McConnell et al. 1998; Roninson et al. 2001; Terao et al. 2001). Recently, stem cell depletion or loss-of-function was proposed as a process that causes organismal aging (Smith and Daniel 2012). As organisms age, hematopoietic stem cells (HSCs) lose their differentiation ability, resulting in decreased bone marrow cellularity and lymphopoiesis and increased myeloid abnormalities (Smith and Daniel 2012; Woolthuis et al. 2011). Replicative stress encompasses both a progressive loss of proliferation capability and a declining differentiation potential of MSCs (Muraglia et al. 2000; Yu and Kang 2013). Therefore, elucidating the senescence mechanism of adult stem cells might provide a clue to link aging at the cellular and organismal levels.

MicroRNAs (miRNAs) are small, non-coding RNAs that are ~22 nucleotides in length and are known to

regulate genes that are important for maintaining clonogenicity and adipogenic differentiation potential or for inducing cellular senescence through the repression of target mRNA translation via complementary binding to the 3' untranslated region (UTR) (Bonifacio and Jarstfer 2010; Liu et al. 2011; Martinez et al. 2011; Yi et al. 2008). The let-7 family of miRNAs inhibits KRAS, HMGA2, and c-MYC expression and induces replicative cellular senescence (Chivukula and Mendell 2008; Grillari and Grillari-Voglauer 2010). The miR15a/16-1 and miR-17-92 clusters are potent regulators of cell cycle progression that target CDK6, CARD10, and CDC27 mRNAs, as well as the CDK inhibitor family members, including p21, p27, and p57 (Chivukula and Mendell 2008; Grillari and Grillari-Voglauer 2010).

In this study, we examined the role of AIMP3/p18 in senescence and in the regulation of clonogenicity and adipogenic differentiation potential in hMSCs. Moreover, we demonstrated that miR-543 and miR-590-3p regulate the senescence phenotype by directly targeting AIMP3/p18 expression during adult stem cell aging.

## Results

Clonogenicity and adipogenic differentiation potential decreased and AIMP3/p18 expression increased in replication-, contact inhibition-, and mitomycin C-induced senescence in hMSCs

To assess the effect of senescence on the clonogenicity and adipogenic differentiation potential of hMSCs, we investigated the changes in hMSC clonogenicity and adipogenic differentiation potential under various senescence conditions. First, we evaluated the direct effects of replication-induced senescence, contact inhibition-induced senescence, and mitomycin C-induced senescence on SA- $\beta$ -gal activity, the colony-forming unit-fibroblast (CFU-F) assay, and the adipogenic differentiation potential. All senescent conditions significantly increased SA- $\beta$ -gal activity, whereas hMSC clonogenicity was compromised (Fig. 1a–c). The adipogenic differentiation potential was reduced under all senescent conditions compared with the control hMSCs, as evidenced by Oil Red O staining (Fig. 1d, e). The expression levels of adipogenic genes, such as C/EBP- $\beta$ , C/EBP- $\delta$ , aP2, and PPAR- $\gamma$ , were significantly down-regulated in all senescent conditions (Fig. 1f). Next, we measured the expression of the CDK

inhibitors p16<sup>INK4A</sup> and p21<sup>CIP1/WAF1</sup>, which are representative aging markers, and assessed the changes in AIMP3/p18 protein expression under each condition (Bringold and Serrano 2000; Lin et al. 1998). We found that the expression of both p16<sup>INK4A</sup> and p21<sup>CIP1/WAF1</sup> increased in replication-, contact inhibition-, and mitomycin C-induced senescent cells, whereas only the expression of p21<sup>CIP1/WAF1</sup> increased in H<sub>2</sub>O<sub>2</sub>-treated cells (Fig. 1g, h, Supplemental Fig. 1 A, B). The expression of AIMP3/p18 increased in senescent cells in which the expression of both p16<sup>INK4A</sup> and p21<sup>CIP1/WAF1</sup> increased. These results suggest that AIMP3/p18 might be involved in replicative senescence and in other p16<sup>INK4A</sup>-associated senescence-inducing conditions, such as mitomycin C treatment and contact inhibition.

## AIMP3/p18 regulates senescence phenotypes in hMSCs

To investigate the role of AIMP3/p18 in adult stem cell aging, we overexpressed AIMP3/p18 in early passage (4–8 passages) hMSCs expressing a low level of AIMP3/p18 or inhibited AIMP3/p18 in late passage (12–18 passages) hMSCs expressing a high level of AIMP3/p18. AIMP3/p18 overexpression in early passage hMSCs increased the expression of p16<sup>INK4A</sup> and p21<sup>CIP1/WAF1</sup> and reduced the proportion of early passage cells in S phase. In contrast, AIMP3/p18 inhibition via multiple transfection of si-AIMP3/p18 during consecutive passages decreased p16<sup>INK4A</sup> and p21<sup>CIP1/WAF1</sup> expression (Fig. 2a, Supplemental Fig. 1c). Moreover, to determine whether senescence markers are affected by AIMP3/p18 during contact inhibition-induced senescence in which AIMP3/p18 is up-regulated, we inhibited AIMP3/p18 expression under these conditions and detected a decrease in p16<sup>INK4A</sup> expression (Supplemental Fig. 2 C).

Next, we investigated senescence phenotypes of hMSCs after AIMP3/p18 overexpression in early passage hMSCs or after AIMP3/p18 inhibition in late passage hMSCs. AIMP3/p18 overexpression in early passage hMSCs increased SA- $\beta$ -gal activity, followed by decreased clonogenic potential, indicating that AIMP3/p18 overexpression is sufficient to induce cellular senescence in hMSCs (Fig. 2b–d). In line with the senescent hMSCs, the AIMP3/p18 up-regulated hMSCs displayed a reduced adipogenic differentiation potential compared with the control hMSCs (Fig. 2h–j). Following AIMP3/p18 inhibition via multiple transfection of si-AIMP3/p18 during consecutive passages,

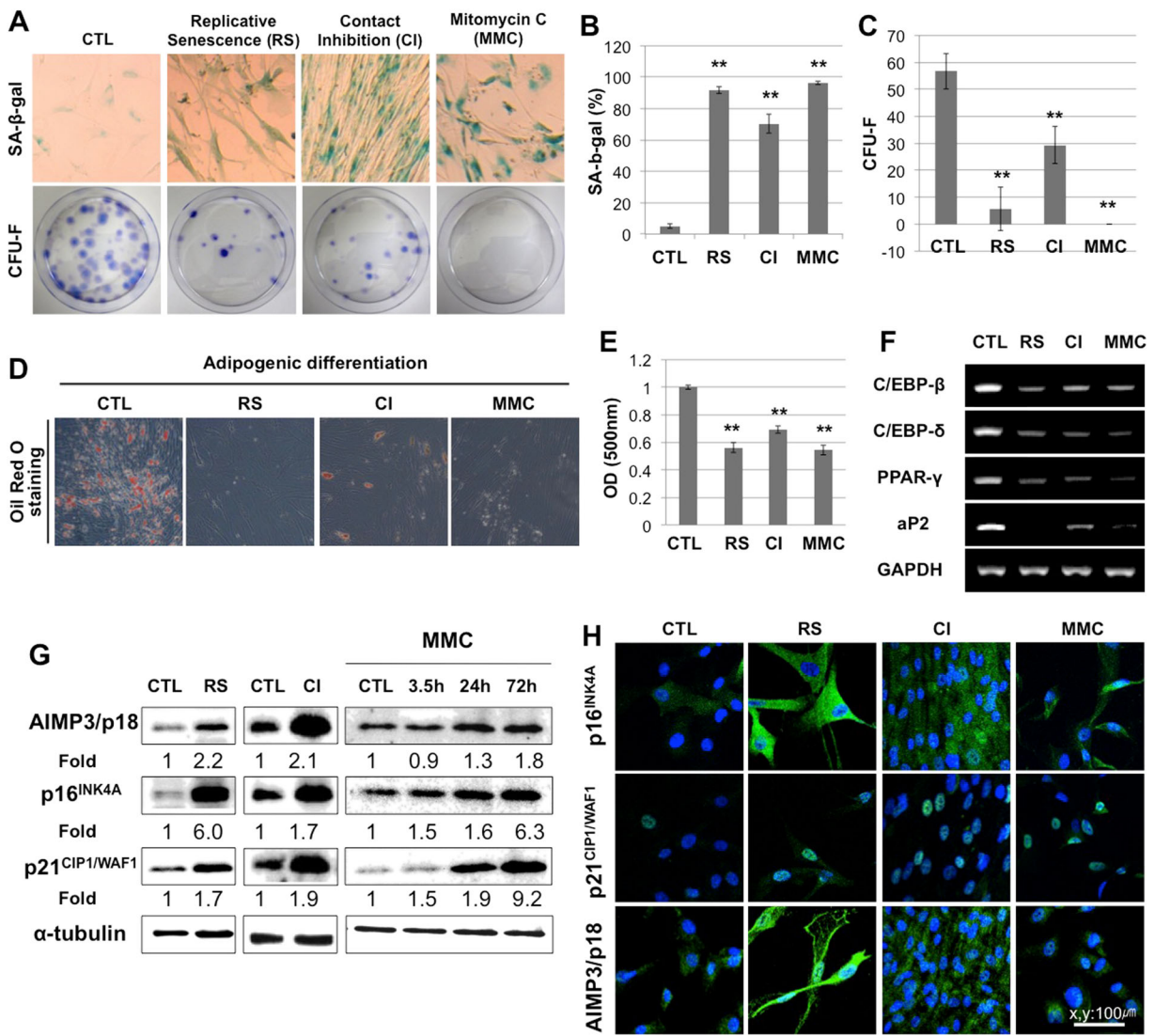


**Fig. 1** The expression level of the AIMP3/p18 protein increased in replicative-, contact inhibition-, and mitomycin C-induced senescent hMSCs. **a** SA-β-gal staining and the CFU-F assay were performed on control and senescent hMSCs. **b** The ratio of SA-β-gal positive cells to total cells is indicated by the graph. **c** The values of CFU-F are indicated by the graph. **d** After adipogenic

differentiation for 3 weeks, lipid droplets were visualized via Oil Red O staining. **e** After eluting the Oil Red O, the absorbance was measured. **f** RT-PCR analysis of the adipogenic markers was performed. **g-h** Expression levels of the AIMP3/p18, p16<sup>INK4A</sup>, and p21<sup>CIP1/WAF1</sup> proteins were confirmed by western blot analysis (**g**) and by immunocytochemistry (**h**). \**P*<0.05; \*\**P*<0.01

AIMP3/p18-inhibited late passage cells displayed a decrease in SA-β-gal positive cells and an increase in colony-forming cells (Fig. 2e-g). The AIMP3/p18-down-regulated hMSCs exhibited increased adipogenic differentiation potential, as evidenced by Oil Red O staining and by the expression of adipogenic transcription factors, including C/EBP-β, C/EBP-δ, aP2, and PPAR-γ (Fig. 2k-m).

Stem cell depletion or loss-of-function was proposed as a process that causes organismal aging (Janzen et al.

2006; Katsara et al. 2011). To investigate whether AIMP3/p18 is involved in the in vivo aging process as well as in vitro aging in MSCs, we isolated and cultured mouse bone marrow-derived mesenchymal stem cells (mBM-MSCs) from 4-week-old (young) and 19-month-old (aged) C57BL/6 mice. The level of Aimp3/p18 expression was higher in the mBM-MSCs from aged mice than that in the mBM-MSCs from young mice (Supplemental Fig. 2a). Consistent with the previous reports, we confirmed that the *Aimp3/p18*TG mice

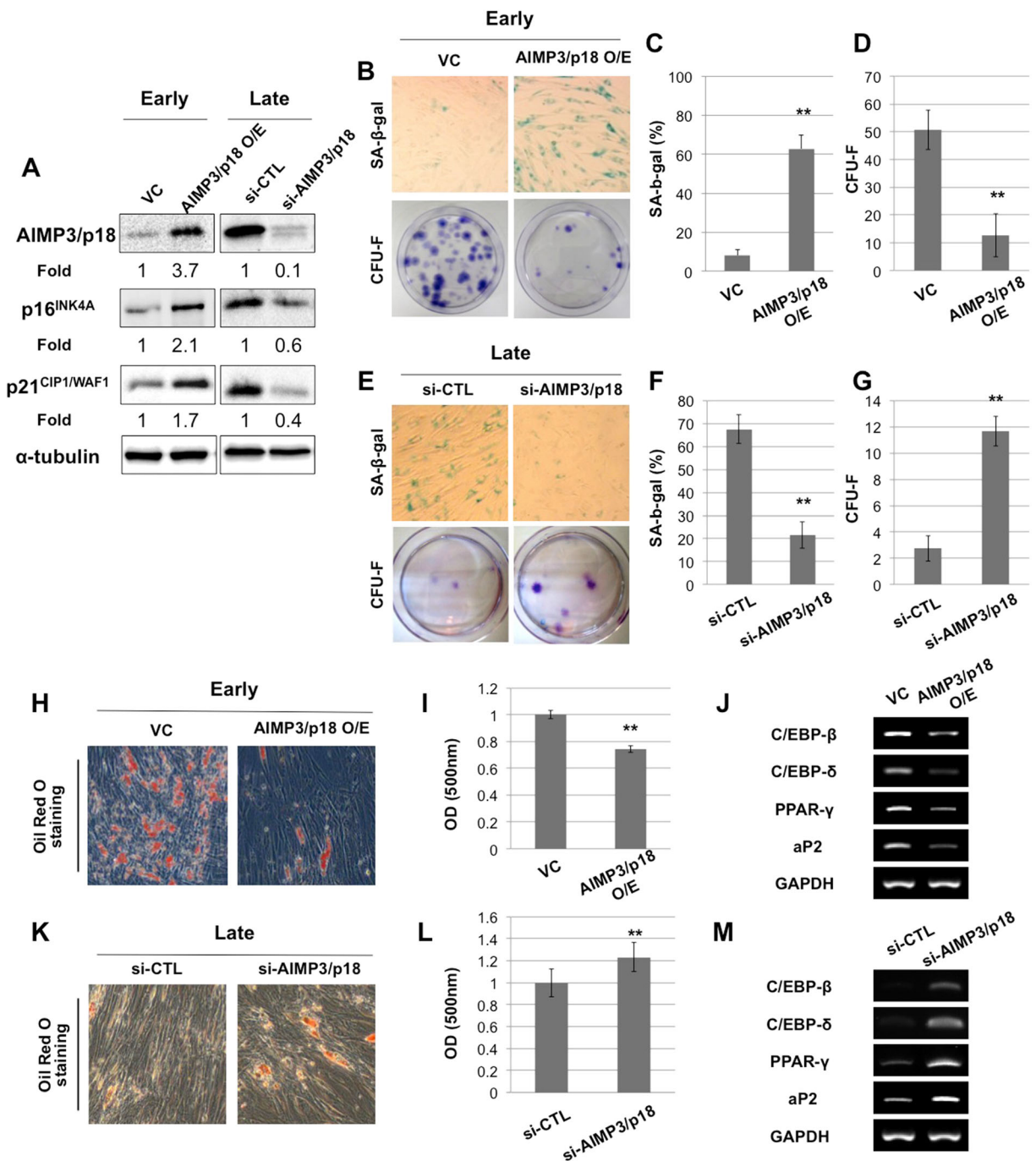


**Fig. 2** AIMP3/p18 regulates cellular senescence and clonogenicity as well as the adipogenic differentiation potential of hMSCs. **a** To up-regulate AIMP3/p18 expression, early passage hMSCs were transfected with 0.5 μg/ml of the AIMP3/p18 expression vector for 48 h. To inhibit AIMP3/p18 expression, late passage hMSCs were transfected with 25 nM siRNA-AIMP3/p18 for 48 h. Protein levels of AIMP3/p18, p16<sup>INK4A</sup> and p21<sup>CIP1/WAF1</sup> were evaluated by western blot analysis. **b** and **e** After

overexpression or inhibition of AIMP3/p18, SA-β-gal staining, and the CFU-F assay were performed. **c** and **f** The ratio of SA-β-gal positive cells to total cells is indicated by the graph. **d** and **g** The values of CFU-F are indicated by the graph. **h** and **k** After adipogenic differentiation for 3 weeks, lipid droplets were visualized using Oil Red O staining. **i** and **l** After eluting the Oil Red O, the absorbance was measured. **j** and **m** RT-PCR analysis of the adipogenic markers was performed. \**P*<0.05; \*\**P*<0.01

displayed a premature aging phenotype and that the senescence markers were increased in the primary organs compared with wild type (WT) mice (Fig. 3a, b, Supplemental Fig. 2b). Furthermore, expression of the senescence markers p16<sup>INK4A</sup> and p21<sup>CIP1/WAF1</sup> was up-regulated in the mBM-MSCs derived from *Aimp3/p18*TG mice compared with WT mice (Fig. 3c). *Aimp3/p18* up-regulation significantly decreased mBM-MSC proliferation and increased SA- $\beta$ -gal activity (Fig. 3d, e). To compare the adipogenic differentiation capacity of the mBM-MSCs between control and *Aimp3/p18* TG mice, we induced the in vitro differentiation of both populations to the adipogenic lineage. The gene expression levels of adipogenic transcription factors, including C/EBP- $\beta$ , aP2, and PPAR- $\gamma$ , were significantly decreased in the mBM-MSCs from *Aimp3/p18* TG mice compared with control mBM-MSCs (Fig. 3f).

miR-543 and miR-590-3p directly target the AIMP3/p18 transcript during hMSC cellular senescence

After elucidating that AIMP3/p18 is up-regulated in senescent hMSCs and that AIMP3/p18 controls senescence markers and phenotypes, we investigated upstream regulators of AIMP3/p18 during hMSC cellular senescence. Recently, we reported that the epigenetic regulators histone deacetylase (HDAC) and DNA methyltransferase (DNMT), as well as miRNAs, are important factors for maintaining stemness and for regulating cellular senescence in hMSCs (Jung et al. 2010; Lee et al. 2011; So et al. 2011). Considering that HDAC and DNMT activities decrease in senescent cells, which corresponds with an increase in the expression of their target genes, we treated hMSCs with the HDAC inhibitors valproic acid (VPA) or sodium butyrate (SB) or with the DNMT inhibitor 5-azacytidine (5-azaC) and then examined the cells for changes in AIMP3/p18 expression. The treated cells displayed a senescence phenotype; however, no increase in the protein levels of AIMP3/p18 was observed (Supplemental Fig. 3A). We also evaluated the expression level of AIMP3/p18 mRNA during senescence-inducing conditions in which the protein level of AIMP3/p18 increased. The mRNA level of AIMP3/p18 did not change significantly under these conditions (Supplemental Fig. 3b). To confirm the changes in the epigenetic status of histone H3 and H4 in the promoter regions of AIMP3/p18, we performed ChIP analysis. The abundance of the transcriptionally

**Fig. 3** AIMP3/p18 controls the expression of senescence markers in mBM-MSCs in vivo. **a** Gross observation of wild-type (WT) and *Aimp3/p18* transgenic (TG) mice. **b** SA- $\beta$ -gal staining and immunohistochemistry for p16<sup>INK4A</sup> in 14-month-old WT and *Aimp3/p18*TG mouse livers. **c** Primary cultures of mBM-MSCs from 10-month-old WT and *Aimp3/p18*TG mice. Protein levels of AIMP3/p18, p16<sup>INK4A</sup>, and p21<sup>CIP1/WAF1</sup> were evaluated by Western blot analysis. **d** The relative growth rate of mBM-MSCs derived from WT and *AIMP3/p18* TG mice was determined using the MTT assay. **e** SA- $\beta$ -gal staining was performed, and the ratio of SA- $\beta$ -gal positive cells to total cells is indicated by the graph. **f** After adipogenic differentiation, RT-PCR analysis of the adipogenic markers was performed

active forms of acetylated histone H4 and H3K4Me3 either did not change or was decreased. The transcriptionally inactive form of H3K27Me3 did not change or was increased under the senescence conditions that increased AIMP3/p18 expression (Supplemental Fig. 3c, d). Based on these results, we hypothesize that AIMP3/p18 regulation during cellular senescence does not occur at the transcriptional but at the post-transcriptional level. Because miRNAs are potent post-transcriptional regulators and because new roles for miRNAs in senescence are continuously being discovered, we focused on identifying novel miRNAs that directly regulate AIMP3/p18 during cellular senescence (Bonifacio and Jarstfer 2010; Martinez et al. 2011). To identify miRNAs that potentially target the 3' UTR of AIMP3/p18 mRNA, we used three periodicity and correlation algorithms: miRanda, PicTar, and TargetScan. We identified 29 predicted AIMP3/p18-targeting miRNAs using miRanda. We chose to pursue the three miRNAs with the highest scores in miRanda, namely miR-590-3p, miR-543, and miR-495, and the two miRNAs that were predicted by all three algorithms, miR-204 and miR-211 (Fig. 4a).

We examined the expression level of the five candidate miRNAs in early and late passage hMSCs using real-time qPCR (Fig. 4b). miR-543 and miR-590-3p expressions were significantly reduced in replication-induced senescent cells. Both miRNAs contain two or three binding sites within the AIMP3/p18 3' UTR (Fig. 4d, Supplemental Fig. 4a), and their seed sequences are conserved among a variety of mammalian species (Supplemental Fig. 4b). Next, we investigated the expression levels of miR-543 and miR-590-3p under additional senescence-inducing conditions. Interestingly, the expression levels of these miRNAs decreased only under conditions in which the AIMP3/p18 protein level was increased (Fig. 4c, Supplemental

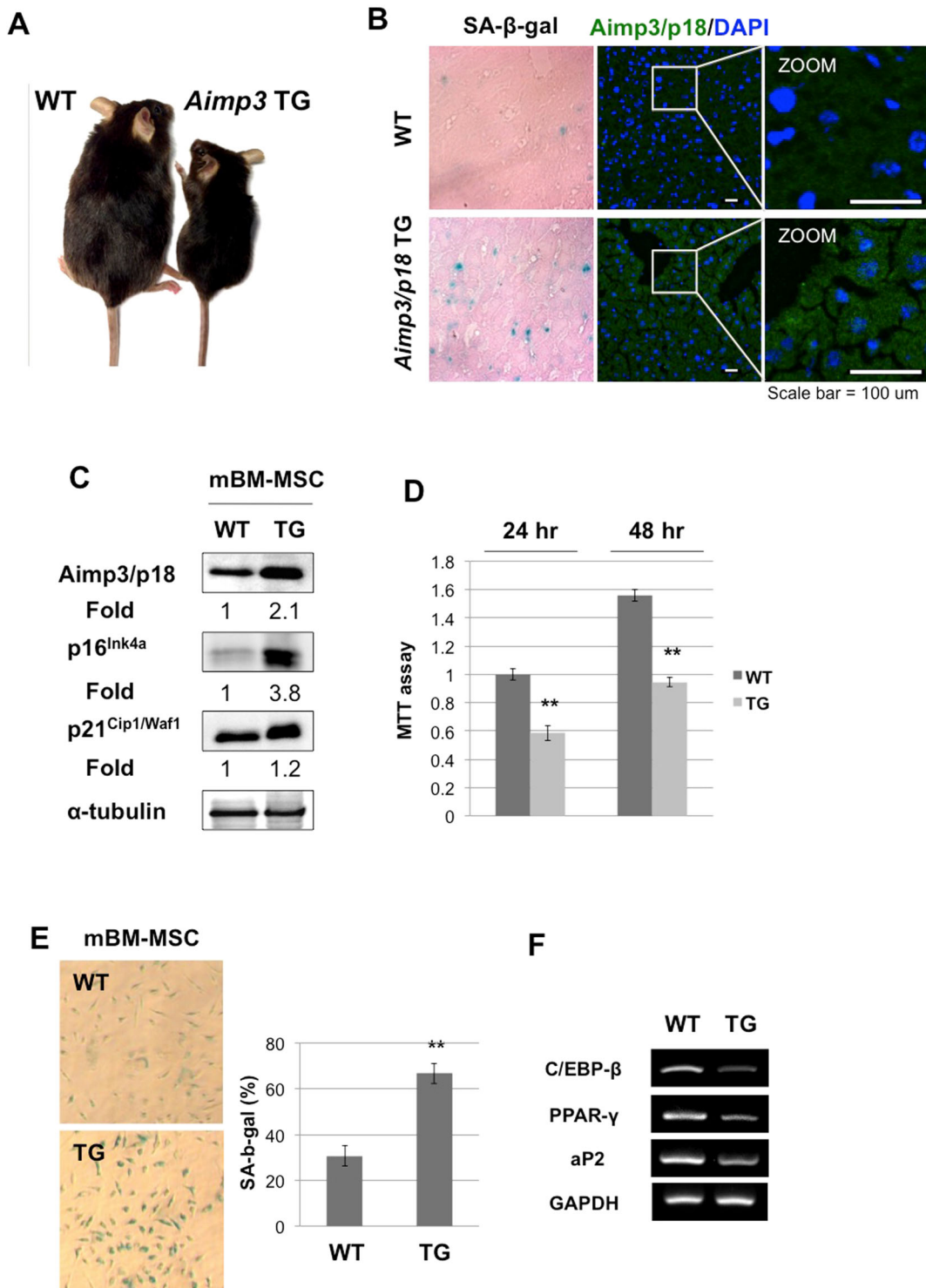
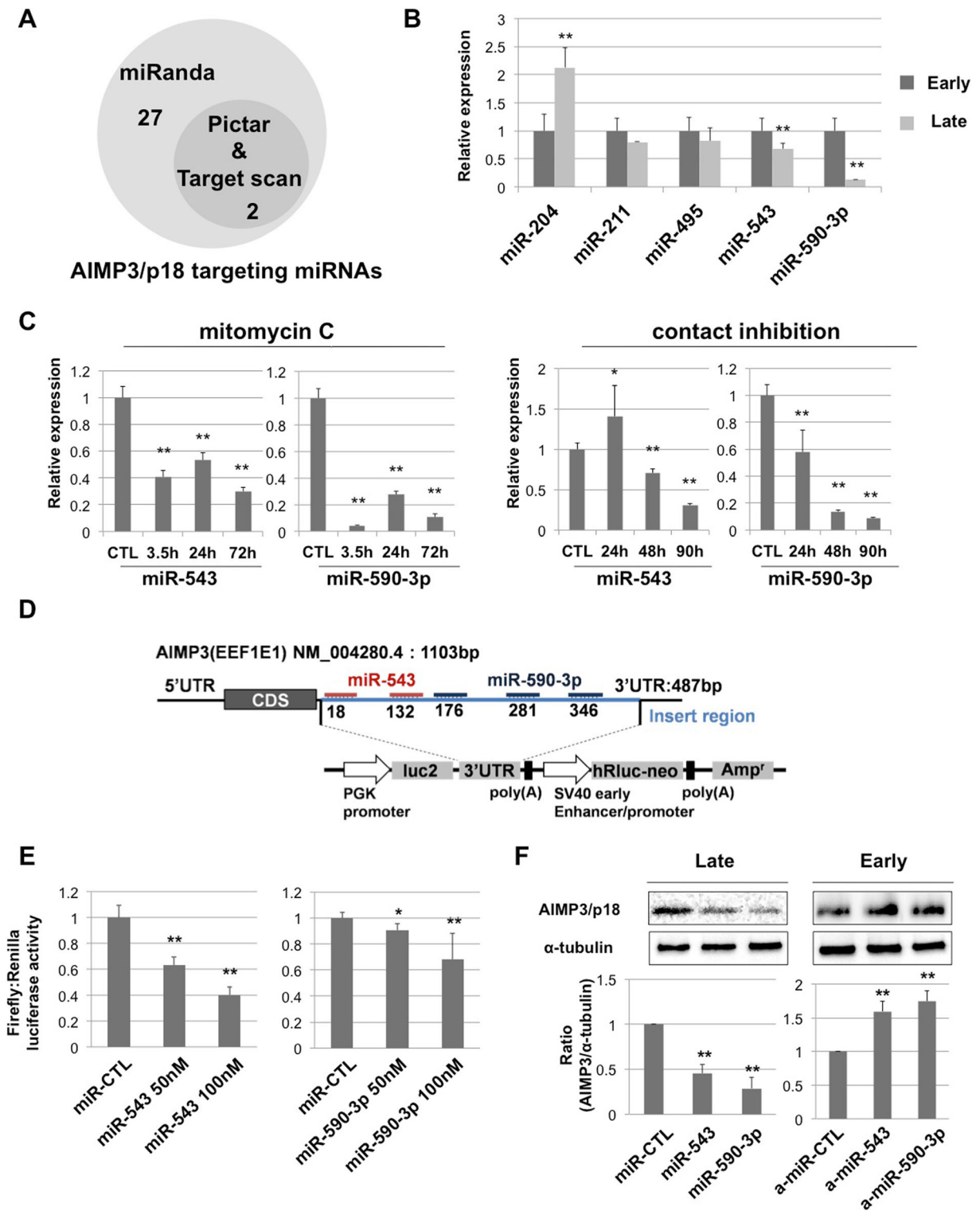


Fig. 4c, d). These results suggest that miR-543 and miR-590-3p are strong candidate upstream regulators of AIMP3/p18 during senescence. To demonstrate the

direct binding of these miRNAs to the AIMP3/p18 3' UTR, we produced an AIMP3/p18 3' UTR luciferase vector that contained the miRNA binding sites, and



293FT cells at 50 % confluency were transfected with this vector. The luciferase activity was significantly

decreased in a dose-dependent manner after transfection with miR-543 or miR-590-3p (Fig. 4e). The

**Fig. 4** miR-543 and miR-590-3p directly target AIMP3/p18. **a** The numbers of predicted AIMP3/p18-targeting miRNAs are shown in the Venn diagram. **b** The expression levels of the five candidate miRNAs were quantified via real-time quantitative PCR. miR-543 and miR-590-3p expressions significantly decreased after replicative senescence. **c** The expression levels of miR-543 and miR-590-3p were confirmed via real-time PCR in mitomycin C- and contact inhibition-induced senescent cells. **d** The expected binding sites of miR-543 and miR-590-3p on the AIMP3/p18 3' UTR region are indicated in the schematic diagram. **e** AIMP3/p18 3' UTR-luciferase assay was performed. AIMP3/p18 3' UTR-luciferase vector and control miRNA (miR-CTL) or mature forms of the miRNA (miR-543 or miR-590-3p) were transfected into 293 T cells. After 48 h, the luciferase assays were performed. The luciferase activities significantly decreased after transfection of the mature form of miR-543 or miR-590-3p in a dose-dependent manner. **f** Late passage hMSCs were transfected with miR-CTL, miR-543, or miR-590-3p. Early passage hMSCs were transfected with anti-miR-CTL, anti-miR-543, or anti-miR-590-3p. Western blot analysis was performed to determine the expression levels of AIMP3/p18 and  $\alpha$ -tubulin. The semi-quantification and visualization of at least three independent assays were performed using ImageJ image analysis software. \* $P < 0.05$ ; \*\* $P < 0.01$

overexpression or inhibition of the miRNAs decreased or increased the protein level of AIMP3/p18, respectively, (Fig. 4f). Moreover, the induction of AIMP3/p18 expression in contact-inhibited cells was reduced in cells transfected with miR-543 or miR-590-3p (Supplemental Fig. 4e). However, the mRNA level of AIMP3/p18 was not regulated by these miRNAs (Supplemental Fig. 4f). These results are consistent with the expression pattern of the AIMP3/p18 protein and mRNA in senescent cells. Taken together, these results indicate that miR-543 and miR-590-3p directly bind to the 3' UTR of AIMP3/p18 mRNA and can be considered upstream regulators of AIMP3/p18 during cellular senescence in hMSCs.

#### miR-543 and miR-590-3p control cellular senescence via AIMP3/p18 regulation

We tested whether the direct regulation of AIMP3/p18 by miRNAs can induce cellular senescence. We inhibited miR-543 and miR-590-3p expression in early passage cells and assessed the gene expression and phenotypic changes (Fig. 5). As expected, the inhibition of these miRNAs via multiple transfection of antisense miRNA during consecutive passages increased the expression of AIMP3/p18 and induced the expression of the senescence markers (Fig. 5a, b). The inhibition of these miRNAs also decreased cell proliferation and clonogenicity, which was confirmed via Ki67 staining

and the CFU-F assay. Furthermore, miR-543 and miR-590-3p inhibition induced SA- $\beta$ -gal activity, as well as decreased cell proliferation and clonogenicity, similar to the phenotypes observed after AIMP3/p18 overexpression (Fig. 5c–f). The miR-543- and miR-590-3p down-regulated hMSCs displayed decreased adipogenic differentiation potential, as evidenced by Oil Red O staining and by the expression of adipogenic transcription factors, including C/EBP- $\beta$ , C/EBP- $\delta$ , aP2, and PPAR- $\gamma$  (Fig. 5g–i).

Next, we transfected hMSCs with the mature forms of miR-543 and miR-590-3p in late passage cells and determined the protein levels of AIMP3/p18 and the senescence markers. The overexpression of these two miRNAs via multiple transfection of either miRNA during consecutive passages decreased the protein expression of AIMP3/p18 and the senescence markers p16<sup>INK4A</sup> and p21<sup>CIP1/WAF1</sup> (Fig. 6a, b). Increased cell proliferation and clonogenicity, as well as decreased SA- $\beta$ -gal activity, was detected after miR-543 or miR-590-3p transfection (Fig. 6c–f). The adipogenic differentiation potential increased in miR-543- and miR-590-3p-transfected hMSCs compared with miR-CTL-transfected hMSCs, as evidenced by Oil Red O staining (Fig. 6g, h). The expression levels of adipogenic genes, such as C/EBP- $\beta$ , C/EBP- $\delta$ , aP2, and PPAR- $\gamma$ , were up-regulated in miR-543- and miR-590-3p-transfected hMSCs (Fig. 6i). Taken together, these data demonstrate that miR-543 and miR-590-3p control cellular senescence through the direct regulation of AIMP3/p18 expression.

## Discussion

Recently, AIMP3/p18 has been reported to be a specific regulator of mature lamin A through proteasome-dependent degradation (Oh et al. 2010). However, whether AIMP3/p18 is increased in senescent cells and plays a role in the stem cell aging process remains unknown. In this study, we determined that AIMP3/p18 expression is up-regulated in replicative senescence, contact inhibition-induced senescence, and mitomycin C-induced senescence hMSCs and controls the progression of the senescent phenotype and the expression of senescence markers under senescence-inducing conditions. Interestingly, H<sub>2</sub>O<sub>2</sub> did not induce an alteration in AIMP3/p18 expression. Kwon et al. reported that UV irradiation induces the release of AIMP3/p18

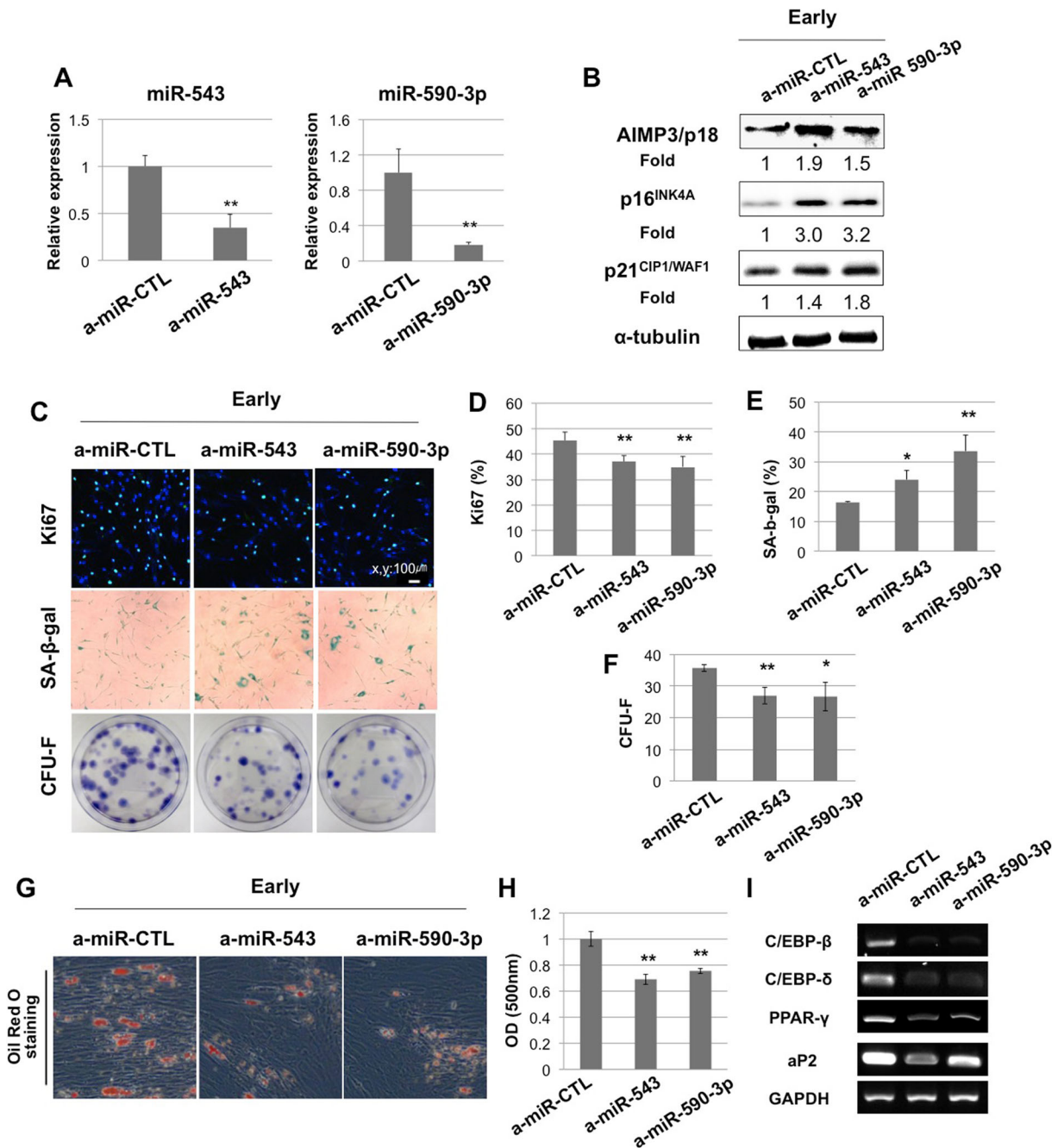


**Fig. 5** miR-543/miR-590-3p inhibition controls hMSC senescence. Early passage hMSCs were transfected with 50 nM anti-miR-CTL, miR-543, or miR-590-3p for 48 h. **a** The expression level of each miRNA was decreased after antisense miRNA transfection. **b** After the transfection of antisense miRNAs, AIMP3/p18, p16<sup>INK4A</sup>, and p21<sup>CIP1/WAF1</sup> protein expression increased, as shown by western blot analysis. **c** Immunocytochemistry for Ki67,

SA- $\beta$ -gal staining, and the CFU-F assay were performed. **d-f** The ratios of Ki67 and SA- $\beta$ -gal positive cells to total cells and the values of CFU-F are indicated by the graphs. **g** After adipogenic differentiation for 3 weeks, lipid droplets were visualized using Oil Red O staining. **h** After eluting the Oil Red O, the absorbance was measured. **i** RT-PCR analysis of the adipogenic markers was performed. \* $P < 0.05$ ; \*\* $P < 0.01$

from MRS, and its translocation to the nucleus for DNA repair upon DNA damage but does not change the

overall amount of AIMP3/p18 (Kwon et al. 2011). Because H<sub>2</sub>O<sub>2</sub> also induces DNA damage, H<sub>2</sub>O<sub>2</sub>

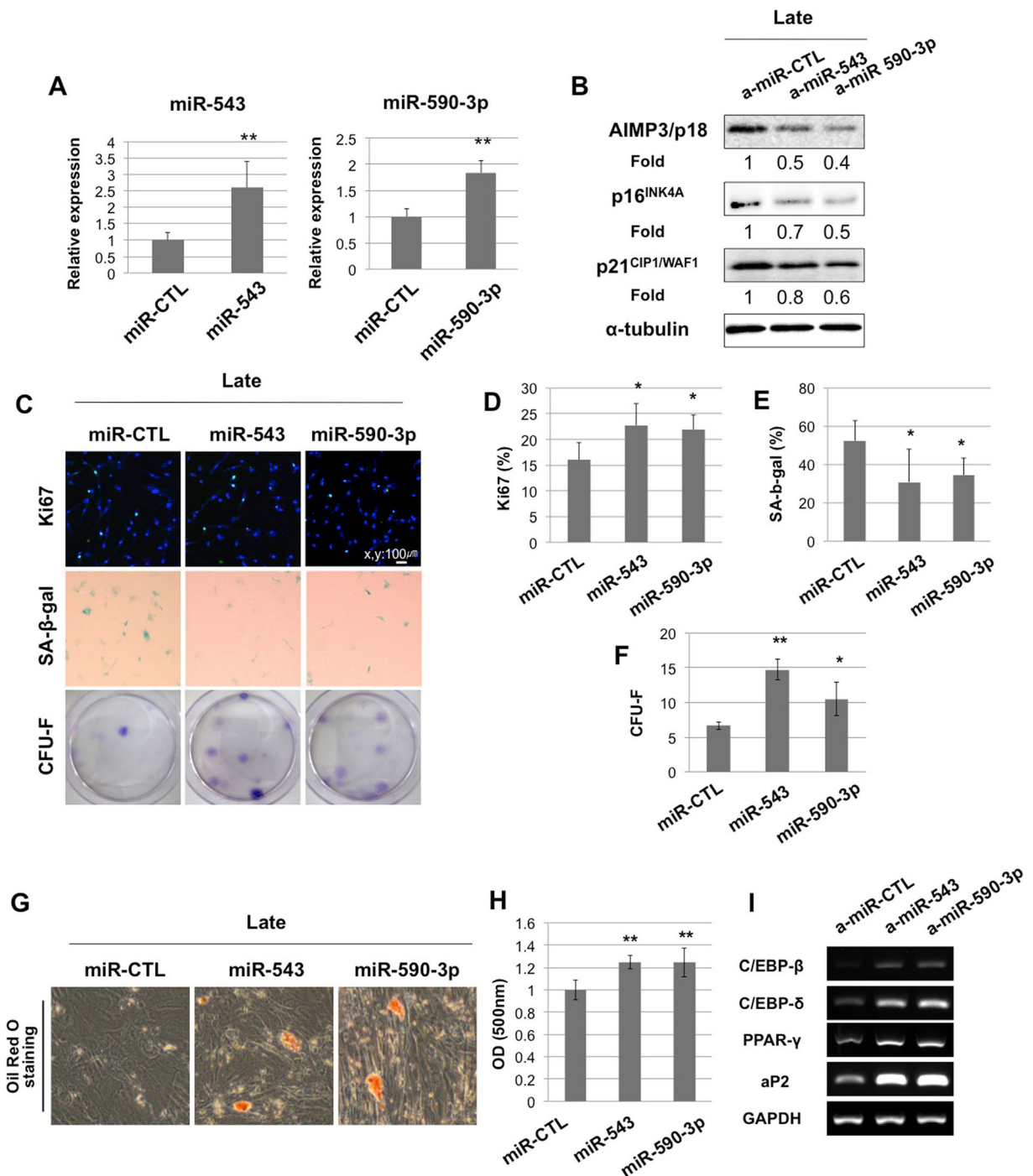


**Fig. 6** miR-543/miR-590 overexpression controls hMSC senescence late passage hMSCs were transfected with 50 nM mature miR-control, miR-543, or miR-590-3p for 48 h. **a** The expression level of each respective miRNA increased after transfection. **b** After the transfection of miRNA, AIMP3/p18, p16<sup>INK4A</sup>, and p21<sup>CIP1/WAF1</sup> protein expression decreased, as shown by western blot analysis. **c** Immunocytochemistry for Ki67, SA- $\beta$ -gal

staining, and the CFU-F assay were performed. **d–f** The ratios of Ki67 and SA- $\beta$ -gal positive cells to total cells and the values of CFU-F are indicated by the graphs. **g** After adipogenic differentiation for 3 weeks, lipid droplets were visualized using Oil Red O staining. **h** After eluting the Oil Red O, the absorbance was measured. **i** RT-PCR analysis of the adipogenic markers was performed. \* $P < 0.05$ ; \*\* $P < 0.01$

treatment may induce an AIMP3/p18 response similar to that of UV irradiation (Driessens et al. 2009).

hMSCs lose their proliferation ability as these cells undergo senescence (Galderisi et al. 2009; Yu and Kang 2013). Furthermore, many reports have consistently found that the adipogenic differentiation potential of hMSCs decreased throughout cellular senescence (Bonab et al. 2006; Fehrer and Lepperdinger 2005; Schellenberg et al. 2011; Wagner et al. 2008). Based on these reports, we investigated the role of AIMP3/p18 in the clonogenicity, adipogenic differentiation ability, and senescence of hMSCs. For the first time, we demonstrated that senescence-induced AIMP3/p18 compromised the clonogenicity and adipogenic differentiation potential of hMSCs. Moreover, the forced expression of AIMP3/p18 in vitro and in vivo also displayed a consistent pattern. In line with the reduced body weight and subcutaneous fat of *Aimp3/p18*TG mice (Oh et al. 2010), *Aimp3/p18* TG mBM-MSCs exhibited retarded growth and adipogenic differentiation ability. The observations that AIMP3/p18 increases under aging-related conditions and that AIMP3/p18 overexpression is sufficient to induce cellular senescence suggest that AIMP3/p18 is both a marker and a regulator of hMSC aging, clonogenicity, and adipogenic differentiation potential.

Although we found that AIMP3/p18 controls hMSC senescence, the downstream mechanism of AIMP3/p18-dependent regulation of aging is not fully understood. We found that the change in AIMP3/p18 expression is coincident with the changes in the expression of the senescence marker p16<sup>INK4A</sup> under senescence conditions. AIMP3/p18 further regulates p16<sup>INK4A</sup> expression based on gain- and loss-of-function studies. Oh et al. reported that the decrease in LMNA caused by the forced expression of AIMP3/p18 is related to the premature aging phenomenon (Oh et al. 2010). Park et al. reported that AIMP3/p18 functions as a tumor suppressor by the Ras-dependent induction of p53 (Park et al. 2006). In our study, we found that p16<sup>INK4A</sup> expression is regulated by AIMP3/p18 in the Tera-1 or PC3 cell lines, which do not express LMNA or p53, respectively (Supplemental Fig. 2 d, e). According to the previous reports and to our data, AIMP3/p18 might regulate cellular senescence through multiple pathways. Further studies are required to identify the exact downstream mechanism of AIMP3/p18 in hMSC cellular senescence.

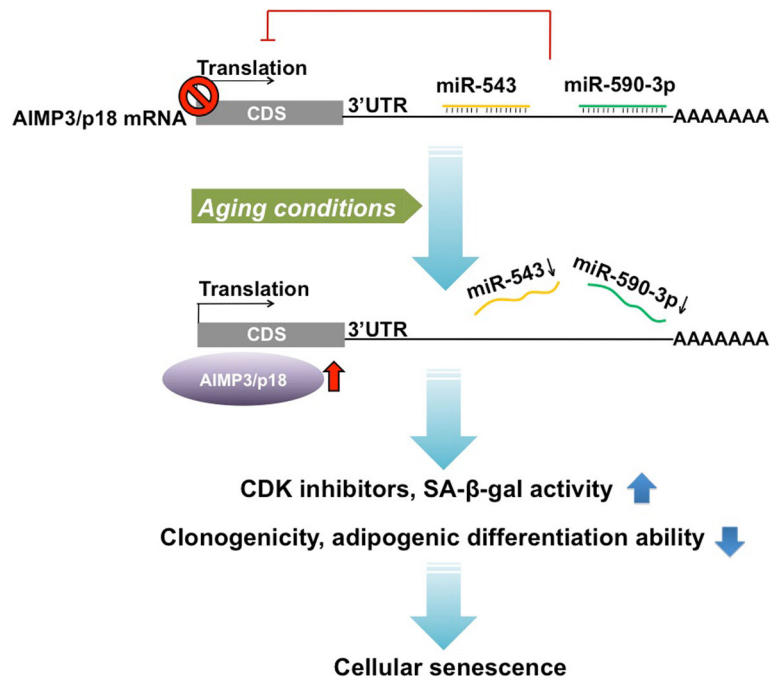
Three known mechanisms of post-transcriptional regulation via miRNAs exist: site-specific cleavage, mRNA degradation, and translational inhibition.

Translational inhibition was first observed for the lin-4 miRNA, which reduced the amount of lin-14 protein without reducing the amount of lin-14 mRNA (Gu and Kay 2010; Valencia-Sanchez et al. 2006; Wightman et al. 1993). Additional examples of miRNA-mediated silencing of target genes without a significant decrease in the mRNA level of these genes have been described (Brennecke et al. 2003; Chen 2004; Cimmino et al. 2005; Gu and Kay 2010; Poy et al. 2004; Valencia-Sanchez et al. 2006). We found no significant change in AIMP3/p18 mRNA expression or chromatin modification, suggesting that AIMP3/p18 regulation is post-transcriptional during the aging process (Supplemental Fig. 3). We found two novel regulators of AIMP3/p18, namely miR-543 and miR-590-3p, which directly target the 3' UTR of AIMP3/p18 mRNA. These miRNAs decreased AIMP3/p18 protein expression but not mRNA expression, supporting the notion that these miRNAs regulated AIMP3/p18 expression not via mRNA cleavage or degradation but rather via translational repression during the aging process.

Recently, miRNAs, which are important regulatory factors due to their potent regulation of target genes, have been shown to be novel modulators of senescence, aging, and longevity (Grillari and Grillari-Voglauer 2010; Liu et al. 2011). However, thus far, no direct target of miR-543 and miR-590-3p has been reported, and only one target, hnRNP-A1, has been predicted for miR-590-3p in Alzheimer's disease patients (Villa et al. 2011). According to our results, AIMP3/p18 induces cellular senescence, miR-543, and miR-590-3p regulate AIMP3/p18 expression, and a significant similarity exists between the phenotypes of the AIMP3/p18-overexpressing and the antisense miRNA-transfected hMSCs. These results suggest that AIMP3/p18 might be the primary downstream effector of these miRNAs in the control of cellular senescence. However, miRNAs frequently have multiple target genes, and mRNAs are generally regulated by multiple miRNAs (Pillai 2005). Therefore, further studies are required to identify additional targets of these miRNAs that may be involved in regulating the mechanism of senescence.

Taken together, our data suggest that AIMP3/p18 is a novel regulator of the aging process in hMSCs. Moreover, we identified miR-543 and miR-590-3p as novel regulators of AIMP3/p18 during cellular senescence (Fig. 7). Because our result is not limited to cellular aging but can be extended to organismal aging, we suggest that AIMP3/p18 and these miRNAs could

**Fig. 7** Schematic diagram describing the regulation of AIMP3/p18 and the mechanism by which AIMP3/p18 controls cellular senescence. AIMP3/p18 is inhibited by miR-543 and by miR-590-3p and is maintained at a low level of expression in young cells. After exposure to senescence-inducing stress, the expression levels of miR-543 and miR-590-3p decrease, and the translational activity of AIMP3/p18 mRNA increases. The increase in AIMP3/p18 expression induces an increase in CDK inhibitors, including p16<sup>INK4A</sup> and p21<sup>CIP1/WAF1</sup>, which is followed by cellular senescence



be novel markers of biological aging. AIMP3/p18 is a known tumor suppressor; therefore, the miRNAs that target AIMP3/p18 might be candidates for cancer therapy or molecular diagnosis and warrant further investigation.

## Materials and methods

### Isolation and culture of MSCs

For the isolation of hMSCs, umbilical cord blood (UCB) samples were obtained from the umbilical vein immediately after delivery, with the written informed consent of the mother. The informed consent form was approved by the Boramae Hospital Institutional Review Board (IRB) and by the Seoul National University IRB (IRB No.1109/001-006). The hMSCs were isolated and cultured as previously described (Yu et al. 2012). Briefly, the UCB samples were mixed with HetaSep solution (StemCell Technologies, Vancouver, Canada) at a ratio of 5:1 and incubated at room temperature to deplete the erythrocytes. The supernatant was carefully collected, and mononuclear cells were obtained using Ficoll density-gradient centrifugation at 2500 rpm for 20 min. The cells were washed twice in PBS. The cells were seeded at a density of  $2 \times 10^5$  to  $2 \times 10^6$  cells/cm<sup>2</sup> on

plates in growth media that consisted of D-media (Formula No. 78-5470EF, Invitrogen, USA) containing EGM-2 SingleQuot and 10 % fetal bovine serum (Invitrogen, USA). After 3 days, non-adherent cells were removed.

For isolating the mBM-MSCs, the soft tissues around the femurs and tibiae of mice were detached. After cutting the end of the diaphysis, the bone marrow was flushed with 15 ml of mouse culture media (low-glucose DMEM containing 20 % FBS and 1 % PS, Invitrogen, USA) using a 25 gauge needle attached to a 1 cc syringe and then filtered through a 40-mm nylon cell strainer (BD Falcon, USA). The cells in the media were centrifuged at 1500 rpm for 5 min, and the pellet was resuspended in 1 ml of red blood cell lysis buffer (Sigma-Aldrich, USA) for 1 min. The cells were centrifuged again with a 10× volume of PBS. The cells were seeded into 6-well plates at a concentration of  $2.5 \times 10^7$  cells/well and cultured at 37 °C in 5 % CO<sub>2</sub>. After 48 h, the cells were washed three times with PBS to remove unattached cells, and the medium was changed.

### Mitomycin C treatment and hydrogen peroxide treatment

Mitomycin C stock solution (0.5 mg/ml, Sigma-Aldrich, USA) was directly added to the culture media at 70 %

confluency to achieve a final concentration of 10 µg/ml. After 3 h of incubation, the cells were washed twice with PBS and changed to fresh culture media. A 30 % hydrogen peroxide solution (Sigma-Aldrich, USA) was diluted in the culture media to achieve a final concentration of 400 µM.

#### Senescence-associated β-galactosidase (SA-β-gal) staining

For analyzing SA-β-gal activity in cells, an X-gal stock solution (4 % X-gal in dimethylformamide, Amresco, USA) was diluted in pre-warmed X-gal dilution buffer (1:40, 5 mM potassium ferricyanide, 5 mM potassium ferrocyanide, and 2 mM magnesium chloride in PBS, pH 6.0). MSCs were washed twice with PBS, fixed with 0.5 % glutaraldehyde (Sigma-Aldrich, USA, diluted in PBS) for 5 min at room temperature and then washed three times with PBS containing 1 mM MgCl<sub>2</sub>. The plates were incubated at 37 °C in the X-gal mixed solution. After 24 h, the cells were washed twice with PBS, and images were acquired using a microscope (IX70, Olympus, Japan).

#### CFU-F assay

For the CFU-F assay, hMSCs were expanded and harvested using trypsin-EDTA. The cells were diluted in cell culture medium and plated at 100 cells/100-mm tissue culture dish. The cells were incubated for 10–14 days at 37 °C in a humidified 5 % CO<sub>2</sub> incubator. To visualize the colonies, the cells were washed with PBS twice and fixed with 5 ml methanol (100 %) for 5 min. After fixation, the cells were dried thoroughly and stained with Giemsa staining solution for 5 min. The cells were washed three times with distilled water, and visible colonies with a diameter greater than 3 mm were counted.

#### Adipogenic differentiation assay

The *in vitro* differentiation of hMSCs into an adipogenic lineage was performed as described previously (Lee et al. 2009; Yu et al. 2012). hMSCs were initially plated in six-well plates, and vectors or microRNAs were transfected for two or three passages. For adipogenic differentiation, cells were treated with an adipogenic medium (DMEM supplemented with 10 % FBS, 1 µM dexamethasone, 10 µM insulin, 200 µM indomethacin,

and 0.5 mM isobutylmethylxanthine) when the confluency reached 80–90 %. Media were changed every 3 or 4 days. Intracellular lipid accumulation, which is an indicator of adipogenic differentiation, was visualized via Oil Red O staining. After photographing, the Oil Red O was eluted with 100 % isopropyl alcohol and quantified using an ELISA plate reader at OD 500.

The *in vitro* differentiation of mBM-MSCs into an adipogenic lineage was performed as described previously (Galderisi et al. 2009). mBM-MSCs were initially cultured in growth medium. For adipogenic differentiation, mBM-MSCs were treated with an adipogenic medium (DMEM supplemented with 10 % FBS, 10 nM dexamethasone, and 17 µM insulin) when the confluency reached 80–90 %. Media were changed every 3 or 4 days.

#### Measurement of cell cycle distribution

Flow cytometry cell cycle analysis using propidium iodide staining was performed as previously described (Rong et al. 2007). Briefly, at least 2 × 10<sup>6</sup> cells were harvested via trypsinization, centrifuged at 1500 rpm for 5 min, and washed with PBS. The cells were centrifuged again and then fixed in 1 ml 70 % EtOH at –20 °C for 1 h. The cells were centrifuged in a 10× volume of PBS at 1500 rpm for 10 min. The supernatant was carefully removed, and the cells were resuspended in 400 µl PBS. Then, 0.05 mg/ml propidium iodide and 6.5 µg/ml RNase A (Invitrogen, USA) were added to stain the cells. After at least 30 min at 37 °C, cell cycle distribution was analyzed using a FACSCalibur system (Becton Dickinson, Franklin Lakes, NJ, USA). All experiments were performed at least three times.

#### Measurement of proliferation potential

The effect of AIMP3/p18 overexpression on mBM-MSC proliferation was measured using the 3-(4,5-dimethylthiazol-2-yl)-2,5-diphenyltetrazolium bromide (MTT, Sigma-Aldrich, St. Louis, MO, USA) assay. mBM-MSCs were plated on 24-well plates at a density of 1 × 10<sup>5</sup>/ml and cultured for 24 or 48 h. At the end of the incubation, 50 µl of MTT stock solution (5 mg/ml) was added, and the plates were further incubated for 4 h at 37 °C. Then, 500 µl dimethyl sulfoxide was added to solubilize the formazan crystals, and the absorbance was measured with an EL800 microplate reader (Bio-Tek

Instruments, USA). All measurements were performed in triplicate.

#### Western blot analysis

The cells were lysed with protein lysis buffer (Pro-PREP, Intron Biotechnologies, Korea), and mouse tissues were homogenized using TissueLyser II (QIAGEN, Germany) for 1.5 min in protein lysis buffer. Prepared proteins were quantified according to Lowry's method, separated via 15 % SDS-PAGE and then transferred to nitrocellulose membranes at 250 mA for 4 h. The primary antibodies used to detect each protein were AIMP3/p18 (1:1000, polyclonal, Abcam, UK), p16<sup>INK4A</sup> (1:1000, polyclonal, Abcam, UK), p21<sup>WAF1/CIP1</sup> (1:1000, polyclonal, Santa Cruz, CA),  $\alpha$ -Tubulin (1:5000, polyclonal, Abcam, UK), and  $\beta$ -Actin (1:2000, polyclonal, Abcam, UK). All antibodies were used according to the manufacturer's instructions, and the protein bands were detected using an enhanced chemiluminescence detection kit (Amersham Pharmacia Biotech, UK) and a FluorChem HD2 imager (Alpha Innotech, San Leandro, CA).

#### Immunocytochemistry

Immunocytochemical analyses of AIMP3/p18, p16<sup>INK4A</sup>, p21<sup>WAF1/CIP1</sup>, and Ki67 were performed. MSCs were fixed in 4 % paraformaldehyde and permeabilized with 0.5 % Triton X-100 (Sigma-Aldrich, USA) for 10 min at room temperature. Then, the cells were incubated in 5 % normal goat serum (Zymed Laboratories Inc., USA) and stained overnight with antibodies against AIMP3/p18 (1:200, polyclonal, Abcam, UK), p16<sup>INK4A</sup> (1:200, polyclonal, Abcam, UK), p21<sup>WAF1/CIP1</sup> (1:200, polyclonal, Santa Cruz, CA), and Ki67 (1:200, polyclonal, Abcam, UK). Next, the cells were incubated for 1 h with an Alexa 488-labeled secondary antibody (1:1000; Molecular Probes, USA). The nuclei were stained with DAPI (Invitrogen, USA), and images were acquired using a confocal microscope (Eclipse TE200, Nikon, Japan).

#### RT-PCR and real-time quantitative PCR

Total cellular RNA was extracted from cells using TRIzol reagent (Invitrogen, USA) according to the manufacturer's instructions. Complementary DNAs (cDNAs) were synthesized by adding purified RNA

and oligo-dT primers to the Accupower RT premix (Bioneer, Korea). cDNAs from miRNAs were synthesized using an NCode VILO miRNA cDNA Synthesis Kit (Invitrogen, USA) according to the manufacturer's instructions. Real-time quantitative PCR was performed using SYBR Green (Applied Biosystems, USA) according to the manufacturer's protocol. RPL13A was used as an internal control. All amplicons were analyzed using a 7500 real-time PCR System (Applied Biosystems, USA). PCR was conducted using the Accupower PCR premix (Bioneer). All PCR products were analyzed via gel electrophoresis on 1.5 % agarose gels with ethidium bromide staining, followed by fluorescence digitization using a Bio-Rad GelDoc XR system (Bio-Rad). The sequences of the primer sets used for this study are provided in Table S1.

#### Transfection

The PC3 DNA control and PC3-AIMP3/p18 expression vectors were generously provided by Sung-hoon Kim (Center for Medicinal Protein Network and Systems Biology, College of Pharmacy, Seoul National University). The FuGENE 6 transfection reagent (Roche, Germany) was used for PC3 control DNA and AIMP3/p18 expression vector transfections according to the manufacturer's instructions. Briefly, when the hMSCs reached 50~60 % confluency, these cells were washed twice with PBS and transfected with 0.5  $\mu$ g/ml vector for 24 to 48 h in fresh culture medium. The DharmaFECT 1 Transfection reagent (Dharmacon, USA) was used for the transfection of small interfering RNA (siRNA), miRNA, or anti-miRNA (Bioneer, Korea) according to the manufacturer's instructions. The siRNA sequence to AIMP3/p18 was 5'-CCAAGU CUAACAGGAUUGACUACUA-3'. When the hMSCs reached 50~60 % confluency, these cells were washed twice with PBS and transfected with siRNA, miRNA, or anti-miRNA for 48 h in media without antibiotics. To increase the efficiency of transfection or to investigate the long-term effects, the transfected cells were subcultured, and the next passage of cells was transfected again in the same manner.

#### 3' UTR-luciferase assay

For miRNA target validation, the entire 3' UTR sequence of human AIMP3/p18 was amplified via PCR and cloned into a TA vector (Promega, Madison, WI,

USA, #A1360). The sequences of the primers used were 5'-CTCGAGCTGTCCATGCCATACAGAAGATC-3' (Forward) and 5'-TTCCCTTTTGGCTTCCTTGGC-3' (Reverse). The 3' UTR was subcloned into a pmirGLO Dual-Luciferase vector (Promega, USA) using the restriction enzymes XhoI and Sall. The 293FT cells or hMSCs were seeded into 24-well plates at 50 % confluence 24 h before transfection. The control constructs and AIMP3/p18 3' UTR reporter constructs were co-transfected with 50 nM of the miRNAs (Bioneer, Korea) using DharmaFECT according to the manufacturer's instructions. After 24 h of transfection, the firefly and Renilla luciferase activities were measured using a luminometer with the Dual-Glo Luciferase Assay System (Promega, USA). The firefly luminescence was normalized to the Renilla luminescence.

#### *Aimp3/p18* transgenic mice

*Aimp3/p18* transgenic mice were kindly provided by Sunghoon Kim (Center for Medicinal Protein Network and Systems Biology, College of Pharmacy, Seoul National University). C57BL/6 wild-type mice were used as a control.

#### Statistical analysis

All experiments were conducted at least three times ( $n=3$ ), and the results are expressed as the mean $\pm$ SD. Statistical analysis was conducted via Student's *t* test. A value of  $p<0.05$  was considered significant.

**Acknowledgments** This research was supported by a grant of the Korea Health Technology R&D Project through the Korea Health Industry Development Institute (KHIDI), funded by the Ministry of Health & Welfare, Republic of Korea (grant number: A120176) and by the Research Institute for Veterinary Science, Seoul National University.

**Conflict of interest** The authors declare no conflicts of interest.

#### References

Blagosklonny MV (2003) Cell senescence and hypermitogenic arrest. *EMBO Rep* 4:358–362. doi:10.1038/sj.embor.embor806

- Bonab MM, Alimoghaddam K, Talebian F, Ghaffari SH, Ghavamzadeh A, Nikbin B (2006) Aging of mesenchymal stem cell in vitro. *BMC Cell Biol* 7:14. doi:10.1186/1471-2121-7-14
- Bonifacio LN, Jarstfer MB (2010) MiRNA profile associated with replicative senescence, extended cell culture, and ectopic telomerase expression in human foreskin fibroblasts. *PLoS One* 5. doi:10.1371/journal.pone.0012519
- Brennecke J, Hipfner DR, Stark A, Russell RB, Cohen SM (2003) Bantam encodes a developmentally regulated microRNA that controls cell proliferation and regulates the proapoptotic gene *hid* in *Drosophila*. *Cell* 113:25–36
- Bringold F, Serrano M (2000) Tumor suppressors and oncogenes in cellular senescence. *Exp Gerontol* 35:317–329
- Chang BD et al (1999) A senescence-like phenotype distinguishes tumor cells that undergo terminal proliferation arrest after exposure to anticancer agents. *Cancer Res* 59:3761–3767
- Chen X (2004) A microRNA as a translational repressor of *APETALA2* in *Arabidopsis* flower development. *Science* 303:2022–2025. doi:10.1126/science.1088060
- Chivukula RR, Mendell JT (2008) Circular reasoning: microRNAs and cell-cycle control. *Trends Biochem Sci* 33:474–481. doi:10.1016/j.tibs.2008.06.008
- Cimmino A et al (2005) miR-15 and miR-16 induce apoptosis by targeting *BCL2*. *Proc Natl Acad Sci U S A* 102:13944–13949. doi:10.1073/pnas.0506654102
- Driessens N et al (2009) Hydrogen peroxide induces DNA single- and double-strand breaks in thyroid cells and is therefore a potential mutagen for this organ. *Endocr-Relat Cancer* 16:845–856. doi:10.1677/ERC-09-0020
- Fehrer C, Lepperdinger G (2005) Mesenchymal stem cell aging. *Exp Gerontol* 40:926–930. doi:10.1016/j.exger.2005.07.006
- Galderisi U et al (2009) In vitro senescence of rat mesenchymal stem cells is accompanied by downregulation of stemness-related and DNA damage repair genes. *Stem Cells Dev* 18:1033–1042. doi:10.1089/scd.2008.0324
- Grillari J, Grillari-Voglauer R (2010) Novel modulators of senescence, aging, and longevity: Small non-coding RNAs enter the stage. *Exp Gerontol* 45:302–311. doi:10.1016/j.exger.2010.01.007
- Gu S, Kay MA (2010) How do miRNAs mediate translational repression? *Silence* 1:11. doi:10.1186/1758-907X-1-11
- Hayflick L (1965) The limited in vitro lifetime of human diploid cell strains. *Exp Cell Res* 37:614–636
- Itahana K, Dimri G, Campisi J (2001) Regulation of cellular senescence by p53. *Eur J Biochem / FEBS* 268:2784–2791
- Janzen V et al (2006) Stem-cell ageing modified by the cyclin-dependent kinase inhibitor p16INK4a. *Nature* 443:421–426. doi:10.1038/nature05159
- Jung JW, Lee S, Seo MS, Park SB, Kurtz A, Kang SK, Kang KS (2010) Histone deacetylase controls adult stem cell aging by balancing the expression of polycomb genes and jumonji domain containing 3. *Cell Mol Life Sci* : CMLS 67:1165–1176. doi:10.1007/s00018-009-0242-9
- Kang T et al (2012) AIMP3/p18 controls translational initiation by mediating the delivery of charged initiator tRNA to initiation complex. *J Mol Biol* 423:475–481. doi:10.1016/j.jmb.2012.07.020
- Katsara O et al (2011) Effects of donor age, gender, and in vitro cellular aging on the phenotypic, functional, and molecular characteristics of mouse bone marrow-derived mesenchymal

- stem cells. *Stem Cells Dev* 20:1549–1561. doi:10.1089/scd.2010.0280
- Kim S, You S, Hwang D (2011) Aminoacyl-tRNA synthetases and tumorigenesis: more than housekeeping *Nature. Rev Cancer* 11:708–718. doi:10.1038/nrc3124
- Kwon NH et al (2011) Dual role of methionyl-tRNA synthetase in the regulation of translation and tumor suppressor activity of aminoacyl-tRNA synthetase-interacting multifunctional protein-3. *Proc Natl Acad Sci U S A* 108:19635–19640. doi:10.1073/pnas.1103922108
- Lee S et al (2011) Histone deacetylase regulates high mobility group A2-targeting microRNAs in human cord blood-derived multipotent stem cell aging *Cellular and molecular life sciences. CMLS* 68:325–336. doi:10.1007/s00018-010-0457-9
- Lee S et al (2009) Histone deacetylase inhibitors decrease proliferation potential and multilineage differentiation capability of human mesenchymal stem cells. *Cell Prolif* 42:711–720. doi:10.1111/j.1365-2184.2009.00633.x
- Lin AW, Barradas M, Stone JC, van Aelst L, Serrano M, Lowe SW (1998) Premature senescence involving p53 and p16 is activated in response to constitutive MEK/MAPK mitogenic signaling. *Genes Dev* 12:3008–3019
- Liu FJ, Wen T, Liu L (2011) MicroRNAs as a novel cellular senescence regulator. *Ageing Res Rev.* doi:10.1016/j.arr.2011.06.001
- Martinez I, Almstead LL, DiMaio D (2011) MicroRNAs and senescence. *Ageing* 3:77–78
- McConnell BB, Starborg M, Brookes S, Peters G (1998) Inhibitors of cyclin-dependent kinases induce features of replicative senescence in early passage human diploid fibroblasts. *Current Biol: CB* 8:351–354
- Muraglia A, Cancedda R, Quarto R (2000) Clonal mesenchymal progenitors from human bone marrow differentiate in vitro according to a hierarchical model. *J Cell Sci* 113(Pt 7):1161–1166
- Oh YS et al (2010) Downregulation of lamin A by tumor suppressor AIMP3/p18 leads to a progeroid phenotype in mice. *Ageing Cell* 9:810–822. doi:10.1111/j.1474-9726.2010.00614.x
- Olovnikov AM (1996) Telomeres, telomerase, and aging: Origin of the theory. *Exp Gerontol* 31:443–448
- Park BJ et al (2005) The haploinsufficient tumor suppressor p18 upregulates p53 via interactions with ATM/ATR. *Cell* 120:209–221. doi:10.1016/j.cell.2004.11.054
- Park BJ, Oh YS, Park SY, Choi SJ, Rudolph C, Schlegelberger B, Kim S (2006) AIMP3 haploinsufficiency disrupts oncogene-induced p53 activation and genomic stability. *Cancer Res* 66:6913–6918. doi:10.1158/0008-5472.CAN-05-3740
- Pillai RS (2005) MicroRNA function: Multiple mechanisms for a tiny RNA? *RNA* 11:1753–1761. doi:10.1261/rna.2248605
- Poy MN et al (2004) A pancreatic islet-specific microRNA regulates insulin secretion. *Nature* 432:226–230. doi:10.1038/nature03076
- Rong Q, Huang J, Su E, Li J, Zhang L, Cao K (2007) Infection of hepatitis B virus in extrahepatic endothelial tissues mediated by endothelial progenitor cells. *Virology* 4:36. doi:10.1186/1743-422X-4-36
- Roninson IB, Broude EV, Chang BD (2001) If not apoptosis, then what? Treatment-induced senescence and mitotic catastrophe in tumor cells. *Drug Resist Updat : Rev Comment Antimicrob Anticancer Chemother* 4:303–313. doi:10.1054/drup.2001.0213
- Schellenberg A et al (2011) Replicative senescence of mesenchymal stem cells causes DNA-methylation changes which correlate with repressive histone marks. *Ageing* 3:873–888
- Smith JA, Daniel R (2012) Stem cells and aging: a chicken-or-the-egg issue? *Ageing Dis* 3:260–268
- So AY, Jung JW, Lee S, Kim HS, Kang KS (2011) DNA methyltransferase controls stem cell aging by regulating BMI1 and EZH2 through microRNAs. *PLoS One* 6:e19503. doi:10.1371/journal.pone.0019503
- Terao Y et al (2001) Sodium butyrate induces growth arrest and senescence-like phenotypes in gynecologic cancer cells *International journal of cancer. J Int Cancer* 94:257–267
- Valencia-Sanchez MA, Liu J, Hannon GJ, Parker R (2006) Control of translation and mRNA degradation by miRNAs and siRNAs. *Genes Dev* 20:515–524. doi:10.1101/gad.1399806
- Villa C et al (2011) Role of hnRNP-A1 and miR-590-3p in neuronal death: Genetics and expression analysis in patients with Alzheimer disease and frontotemporal lobar degeneration. *Rejuvenation Res* 14:275–281. doi:10.1089/rej.2010.1123
- Wagner W et al (2008) Replicative senescence of mesenchymal stem cells: a continuous and organized process. *PLoS One* 3:e2213. doi:10.1371/journal.pone.0002213
- Wightman B, Ha I, Ruvkun G (1993) Posttranscriptional regulation of the heterochronic gene lin-14 by lin-4 mediates temporal pattern formation in *C. elegans*. *Cell* 75:855–862
- Woolthuis CM, de Haan G, Huls G (2011) Aging of hematopoietic stem cells: Intrinsic changes or micro-environmental effects? *Curr Opin Immunol* 23:512–517. doi:10.1016/j.coi.2011.05.006
- Yi R, Poy MN, Stoffel M, Fuchs E (2008) A skin microRNA promotes differentiation by repressing ‘stemness’. *Nature* 452:225–229. doi:10.1038/nature06642
- Yu KR, Kang KS (2013) Aging-related genes in mesenchymal stem cells: a mini-review. *Gerontology* 59:557–563. doi:10.1159/000353857
- Yu KR et al (2012) CD49f enhances multipotency and maintains stemness through the direct regulation of OCT4 and SOX2. *Stem Cells* 30:876–887. doi:10.1002/stem.1052